

Simultaneous bimodal surface acoustic-wave velocity measurement by scanning acoustic force microscopy

G. Behme^{a)} and T. Hesjedal^{b)}

Paul Drude Institute for Solid State Electronics, Hausvogteiplatz 5-7, D-10117 Berlin, Germany

(Received 22 March 2000; accepted for publication 5 June 2000)

We present scanning acoustic force microscopy (SAFM) mixing experiments of differently polarized surface acoustic waves (SAW) with noncollinear propagation directions. The phase velocities of the SAWs are measured at a submicron lateral scale, employing a multimode SAFM that is capable of detecting the wave's normal and in-plane oscillation components. Hereby, the down conversion of the surface oscillations into cantilever vibrations due to the nonlinearity of the tip-sample interaction is utilized. The simultaneous determination of the phase velocities within a microscopic sample area is demonstrated for the mixing of Rayleigh and Love waves on the layered system SiO₂/ST-cut quartz. © 2000 American Institute of Physics. [S0003-6951(00)01831-3]

Over the last 70 years the investigation of elastic and also other properties of crystalline and isotropic solids by means of acoustic waves has been very successful.¹ The determination of the elastic parameters, even for materials with a low crystal symmetry, is provided by standardized procedures that utilize the propagation of bulk acoustic waves along specific crystalline directions.² The investigation of the propagation parameters of surface acoustic waves (SAWs) is especially suited to yield information about layered systems. There, the measurement of laser-induced SAW pulses, in particular their angular and frequency dispersions, allows the very accurate determination of thin film parameters, such as elastic moduli and density.³ Both approaches suffer from demands of the sample geometry. Although very small sample volumes are accessible for resonance techniques,⁴ one is restricted to precisely determined sample shapes. For pulse propagation measurements large and flat sample surfaces are required. Also, an excellent homogeneity of substrate and film is requested. These demands are partly overcome by line focus acoustic microscopy that delivers elastic parameters for a small probe area with excellent accuracy.⁵ The SAW velocity can be measured with an unmatched precision well below 1 ms⁻¹. However, this method is, concerning the change in velocity, not very sensitive to surfaces and thin overlayers because of the operating frequency of 225 MHz. This results in SAW wavelenghts of about ten microns with a similar penetration depth into the volume.

On the other hand, a quite successful approach to thin film properties is to place the material within the propagation path of a SAW device and to measure the change in the electrical transmission. A very rigorous attempt was used for the investigation of superconducting YBa₂Cu₃O_{7- δ} films where the specimen was bridging a gap within a SAW delay line.⁶ Wafer bonding as a promising approach for materials integration delivers particularly interesting model systems. The change in the SAW velocity due to an external direct-

current (dc) voltage within a GaAs/LiNbO₃ hybrid could clearly be extracted from the phase change of the transmitted electrical signal.⁷ Also, fabricating interdigital transducers on a layered (piezoelectric) material or complete coverage of SAW delay lines delivers useful SAW velocity data. This has been exploited for the measurement of the elastic constants of Al_xGa_{1-x}N layers on sapphire substrates.⁸ The most important drawback of these techniques is that only the SAW velocity of one particular SAW mode is available from a single measurement.

Our approach, scanning acoustic force microscopy (SAFM), has been shown to deliver SAW phase velocities with submicron lateral resolution.⁹ In this letter, we present an extended approach that is capable of simultaneously delivering two velocities for differently polarized SAW modes, e.g., for acoustic modes propagating in perpendicular directions. This is achieved in microscopic areas of thin film samples that are located within the propagation path of specific SAW devices.

In conventional SAFM, that is described in detail elsewhere,^{10,11} the additional contributions to the cantilever bending by the interaction between the oscillating surface and the atomic force microscopy (AFM) tip is analyzed. The nonlinearity in the tip-surface interaction, namely the nonlinear force versus distance curve, leads to detectable cantilever deflections as a result of the radio-frequency (rf) surface oscillations of the SAWs. The introduction of two rf fields at slightly detuned frequencies results in detectable oscillation signals at harmonics of the difference frequency, if this frequency is below or near the mechanical cantilever contact resonance. These low-frequency (lf) signals are picked up via the standard lateral force microscopy optical deflection detection, analyzed by a lock-in amplifier, and recorded simultaneously with the AFM scan. A similar mechanism is also in effect for the coupling of purely transverse oscillations into the cantilevers torsional degree of freedom. This allows the analysis of in-plane polarized, i.e., transverse or quasilongitudinal wave modes.¹²

The first SAFM phase velocity measurements of SAWs were achieved using a collinear arrangement of interdigital transducers (IDTs) on ST-cut quartz.⁹ Opposing IDTs were

^{a)}Electronic mail: behme@pdi-berlin.de

^{b)}Author to whom correspondence should be addressed; Current address: Solid State and Photonics Lab, CIS-X, Stanford University, Stanford, California 94305-4075; electronic mail: thornsten@snow.stanford.edu

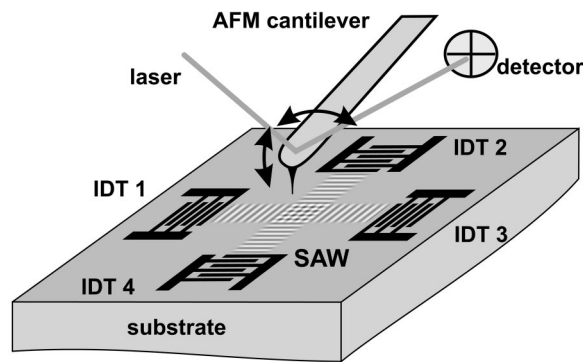


FIG. 1. Sketch of the SAFM experimental setup: detuned rf surface acoustic waves are launched by IDTs on a piezoelectric substrate towards the measurement region, where a down conversion at the tip-sample contact takes place. The resulting vertical and lateral 1f cantilever oscillations are optically detected and analyzed by a lock-in amplifier. Phase and amplitude are recorded along with the topography scan.

used for the excitation of waves with antiparallel wave vectors. Two rf generators power the IDTs at slightly different frequencies. A third phase-locked generator provides the difference frequency signal that is used as the reference for a lock-in amplifier. In first order approximation, the phase of the resulting sinusoidal cantilever oscillation is given by $\varphi = \Delta\omega t - (k_1 - k_2)x$, where $\Delta\omega$ is the difference frequency, k_1 and k_2 the k vectors of the SAWs, and x the coordinate parallel to the wave propagation. As the difference frequency is in the kHz range, i.e., by several orders of magnitude smaller than the operating frequency, the absolute value of the k vectors is almost identical. Thus the spatial rise of the phase signal is given by twice the k vector or $4\pi f/v_{\text{SAW}}$, with v_{SAW} the phase velocity and f the operating frequency.

As a simple model system, the standing wave field between an arrangement of four crossed IDTs (see Fig. 1) was investigated. Rayleigh-type waves were excited by IDTs on (001) GaAs in [110] directions at a working frequency of 198 MHz ($\lambda_{\text{SAW}} = 14.4 \mu\text{m}$). Figure 2(d) shows the SAW amplitude pattern obtained by a mixing experiment using four SAWs, resembling a regular dot pattern. Two rf generators with a frequency difference of 5 kHz were used to power three IDTs. The fourth IDT acts as a reflector for the opposing one. In this direction (along the x axis) the modulation is less pronounced. The image clearly reproduces the features of the standing wave field with the periodicity of $\lambda_{\text{SAW}}/2 = 7.2 \mu\text{m}$ in two spatial directions. The phase image [Fig. 2(c)] strongly deviates from a linear, sawtooth-like behavior due to the multiple contributions to the cantilever oscillation at the difference frequency with different spatial evolution.

The simulated images were obtained from a straightforward numerical simulation under the assumption of planar wave propagation. The results of the nonlinear superposition of the oscillation components at the difference frequency, namely the local phase and amplitude, are shown in Figs. 2(a) and 2(b). As the nonlinear nature of the interaction inhibits the extraction of absolute amplitude information, the parameters for the simulation were arbitrarily chosen for the best correspondence with the experimental results.

Having accomplished the measurement of crossed wave fields of the same SAW type, we investigated samples where different acoustic modes can be launched towards the mea-

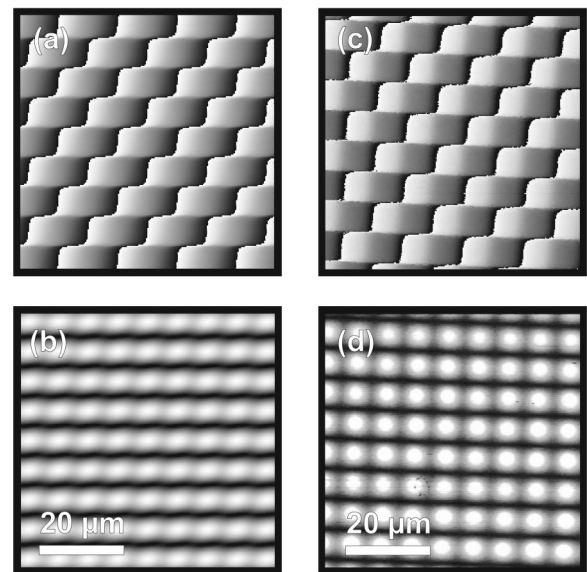


FIG. 2. SAW phase (a),(c) and amplitude (b),(d) patterns of a Rayleigh-type wave field obtained by a SAFM mixing experiment. (a) and (b) show the simulated data and (c) and (d) the experimental data, respectively. Two rf generators were used to power three of the four IDTs, while the fourth is acting as a wave reflector to establish a partly standing wavefield.

surement region. On ST-cut quartz, IDTs were fabricated with an electrode periodicity (SAW wavelength) of $5.6 \mu\text{m}$ in the 0° direction (with respect to the crystal X axis). In this direction, Rayleigh-type SAWs can be excited. Under 90° , transducers with a period of $8.8 \mu\text{m}$ were deposited, which excite surface transverse waves (STW) on the bare substrate. This mode converts into a Love mode when a thin layer with a smaller transverse bulk wave velocity covers its path. It contains only one oscillation component that is oriented in-plane and perpendicular to the propagation direction (see Fig. 3).

The wavelengths were chosen to achieve an overlap in the working frequencies when a SiO_2 layer covers the surface.¹³ This layer lowers the velocity of the excited Love wave, and thus the operating frequency, towards the value of the Rayleigh-type wave. For the actual sample the layer thickness was 190 nm. The IDT center frequencies were 562.8 MHz for the Rayleigh-type wave and 563.1 MHz for the Love wave.

An SAFM mixing experiment was then performed in the region of overlapping SAW beams. Figure 4 shows the simu-

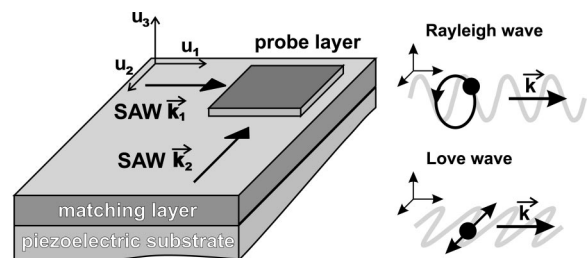


FIG. 3. Sketch of the investigated material system: a matching layer is deposited on top of the piezoelectric substrate and a probe layer is placed in some distance from the IDTs. The wave displacement components (u_1, u_2, u_3) for the two wave types are shown on the rhs.; u_1 is along the propagation direction. The Rayleigh-type wave is predominantly polarized in the $u_1 - u_3$ plane, whereas the Love wave only has an in-plane (u_2) oscillation component.

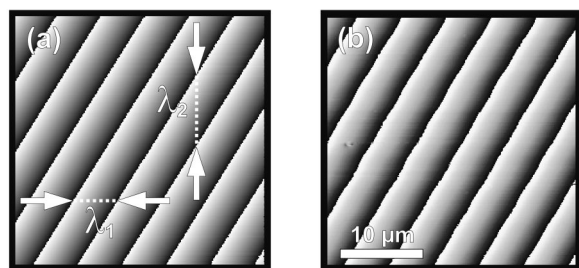


FIG. 4. (a) Simulated and (b) measured SAFM phase image. The mixing experiment was carried out using a Rayleigh-type wave (propagating from right to left) and a Love wave (propagating from top to bottom).

lated (a) and measured phase image (b). The linear phase change was reduced to -180° to 180° intervals by the lock-in amplifier, causing the sawtooth-like behavior. The images were recorded in LFM mode with a resolution of 256×256 points at a scan rate of 0.2 Hz. The propagation directions of the SAWs were from right to left for the Rayleigh wave and top to bottom for the Love wave. The scan area was rotated by 1.3° with respect to the transducer's axis.

As for the collinear geometry, the phase of the cantilever oscillation was determined by the difference of the phase arguments of the incoming SAWs. Thus it becomes $\varphi = \Delta\omega t - k_1x + k_2y$ for two waves propagating under 90° with respect to each other. Obviously, two k vectors can now be simultaneously determined from one measurement. The different wavelengths become visible as phase jump periodicities when following the propagation direction of the SAWs [dotted lines in Fig. 4(a)]. Numerical fitting allows the precise calculation of the spatial rise of the phase and thus the k vectors and the phase velocities of the acoustic waves. The simulation, shown in Fig. 4(a), delivered an ordinary linear phase behavior that was rescaled to the lock-in's 360° data range. The amplitude images (not shown) exhibit no spatial modulation, as only two SAWs were involved.

From these experiments, some conclusions can be drawn concerning the particular nonlinear coupling mechanism. It has been found earlier that the nonlinear coupling of in-plane polarized oscillations into the SAFM signal is at least one order of magnitude less efficient than the corresponding effect for vertical oscillations (in terms of the applied rf power required for high quality phase images). Also, the amplitude of the down-converted signals strongly depends on the surface roughness and tip shape for in-plane oscillations which is less relevant for the vertical coupling. However, having both oscillation components present within the measurement region, the mixing is obtained at lower amplitudes as expected for in-plane only. Also, the influence of tip and surface is reduced. The reason for this behavior is most probably, that the vertical and lateral displacements of Rayleigh and Love wave, sum up to a net displacement, that will point out of the surface. Apparently, the mixing mechanism is thus more of the vertical mechanical diode type.

The wavelengths apparent from Fig. 4(b) are 5.5 and 9.1 μm for the x and y direction, respectively. These values have

to be corrected for the tilt of the scan area. With the working frequency of 562.7 MHz, the phase velocities then become 4940 and 3140 ms^{-1} for the Love- and the Rayleigh-type wave, respectively. We emphasize that both phase velocities were measured simultaneously in the region of interest, which is strongly demanded when elastic properties are to be determined by solving the inverse problem of SAW propagation.¹⁴ Additionally, inherent limitations of the conventional SAFM, like loss of phase resolution due to back-reflections by the opposing transducers, are most elegantly overcome. It should be noted that for ST-cut quartz X -propagation direction not only a Rayleigh wave, but also a transverse pseudo SAW and a quasilongitudinal pseudo SAW may be excited with the same transducer. Also, harmonic operation of the IDTs is possible for Rayleigh and Love waves. Then, of course, different matching layer thicknesses are required for the SAFM investigations. Including these modes will add even more versatility to this approach.

In this letter, we have shown that multimode SAFM can be used to measure differently polarized SAWs with noncollinear propagation directions at a submicron lateral scale. By analyzing the torsion of the cantilever in addition to its bending, normal and in-plane oscillation components due to acoustic waves can be measured. Now, the mixing of the complementary components in crossed wave fields delivers the phase velocities of the involved waves simultaneously at the same sample spot. This enables us, in principle, to investigate the elastic properties of submicron areas through solving the inverse problem of SAW propagation.¹⁴

The authors would like to thank H.-J. Fröhlich for fruitful discussion, F. Jungnickel for the transducer design, and W. Seidel and K. Hauck for the sample preparation. T.H. would like to thank the Leopoldina, Halle, for financial support.

¹F. A. Firestone, U.S. Patent 2,280,226 (1942); J. Krautkrämer and H. Krautkrämer, *Ultrasonic Testing of Materials* (Springer, New York, 1990).

²B. A. Auld, *Acoustic Fields and Waves in Solids* (Krieger, Malabar, FL, 1990).

³J. Maynard, *Phys. Today* **49**, 26 (1996).

⁴*Photoacoustic, Photothermal and Photochemical Processes at Surfaces and in Thin Films*, edited by P. Hess (Springer, Berlin, 1989).

⁵J. Kushibiki and N. Chubachi, *IEEE Trans. Sonics Ultrason.* **SU-32**, 189 (1985).

⁶R. Gaffney, C. Hucho, J. R. Feller, M. J. McKenna, B. K. Sarma, and M. Levy, *Appl. Phys. Lett.* **70**, 1468 (1997).

⁷M. Rotter, C. Rocke, S. Böhm, A. Lorke, A. Wixforth, W. Ruile, and L. Korte, *Appl. Phys. Lett.* **70**, 2097 (1997).

⁸C. Deger, E. Born, H. Angerer, O. Ambacher, M. Stutzmann, J. Hornsteiner, E. Riha, and G. Fischerauer, *Appl. Phys. Lett.* **72**, 2400 (1998).

⁹T. Hesjedal, E. Chilla, and H.-J. Fröhlich, in *1996 Ultrasonics Symposium Proceedings* (IEEE, New York, 1996), p. 811; E. Chilla, T. Hesjedal, and H.-J. Fröhlich, *Phys. Rev. B* **55**, 15852 (1997).

¹⁰W. Röhrbeck and E. Chilla, *Phys. Status Solidi A* **131**, 69 (1992).

¹¹T. Hesjedal, E. Chilla, and H.-J. Fröhlich, *Appl. Phys. A: Solids Surf.* **61**, 237 (1995).

¹²G. Behme, T. Hesjedal, E. Chilla, and H.-J. Fröhlich, *Appl. Phys. Lett.* **73**, 882 (1998).

¹³F. Herrmann and S. Büttgenbach, *Phys. Status Solidi A* **170**, R3 (1998).

¹⁴S. Makarov, E. Chilla, and H.-J. Fröhlich, *J. Appl. Phys.* **78**, 5028 (1995).